https://doi.org/10.5194/nhess-2019-259
Preprint. Discussion started: 23 August 2019
© Author(s) 2019. CC BY 4.0 License.

Natural Hazards and Earth System Sciences
Discussions

Community-based landslide hazard probability and risk assessment: A case in west Hubei, China

Sheng Fu[1], Lixia Chen[1*], Tsehaie Woldai[2], Kunlong Yin[3], Lei Gui[3], Deying Li[3], Juan Du[4], Chao Zhou[5], Yong Xu[6], and Zhipeng Lian[6]

[1] Institute of Geophysics and Geomatics, China University of Geosciences, Wuhan, 430074, China

[2] School of Geosciences, University of Witwatersrand, ZA-2000 Johannesburg, South Africa

[3]Faculty of Engineering, China University of Geosciences, Wuhan, 430074, China

[4]Three Gorges Research Center for Geo-Hazard, Ministry of Education, China University of Geosciences, Wuhan 430074, China

[5]School of Geography and Information Engineering, China University of Geosciences, Wuhan, 430074, China

[6] Wuhan Center of China Geological Survey, Wuhan, 430205, China

Correspondence to: Lixia Chen (lixiachen@cug.edu.cn)

Abstract. Small communities living in high mountainous terrains, in Hubei Province are often impacted by landslide hazard. Past work by China Geology Survey focused only on hazard assessment at 1:100 000 scales. In this study, we conducted a more-detailed semiquantitative landslide and risk assessment at a community level and scale of 1:10 000. We applied the probabilistic method to assess the landslide spatial, temporal and size probabilities while the landslide hazard and risk assessment were considered for four return periods (5, 10, 20 and 50 years) and two size scenarios (landslide volume). The spatial probability by susceptibility mapping with an accuracy of 84% indicates that Quaternary deposits and weathered eluvium from Ordovician limestone are the two major controlling factors. Most building areas in hazard maps are located at the foot of major slopes where hazard probabilities are very high. We computed the loss of lives and properties for each slope. The result shows that 1530 people and 126 million RMB economics were at risk of being affected by landslides with a 50-year return period and a landslide volume of fifty thousand cubic meters.

Meanwhile, the longer the return period, the higher the hazard probability is. Compared with the function by ordinary least square method, classic inverse gamma and power law distribution of landslide magnitude and frequency are not suitable for landslide size probability analysis in the study area. The proposed procedure is proved to be more useful to complement risk assessment on the small scale of 100,000 in west Hubei, China.

Keywords: landslide; hazard probability; element-at-risk; risk assessment; community

https://doi.org/10.5194/nhess-2019-259
Preprint. Discussion started: 23 August 2019
© Author(s) 2019. CC BY 4.0 License.

Natural Hazards and Earth System Sciences Discussions

1 Introduction

Guidelines for landslide risk zoning and land use planning with the framework, definitions and recommendations were provided for different clearly defined scales (Fell et al., 2008a). Also, research work highlighting landslide risks at a community-level has recently been tested, and some of the result reached are open for the public(Abdulwahid and Pradhan, 2016;Chen et al., 2016a;Erener and Düzgün, 2012;Liu et al., 2016;McAdoo et al., 2018;Paliaga et al., 2019). Paliaga et al. (2019), for example, have used a spatial multi-criteria analysis technique (SMCA) to mitigate geo-hydrological risk in a small but densely-populated catchment, with descriptive parameters of the extent of urban development and elements at risk. In Spain, a quantitative assessment of landslide risk for the road network of the Basque Country was used for calculating hazard probability and expected consequences (Mavrouli et al., 2019).

Many investigators in China believe risk analysis and assessment to be an effective means of reducing casualties and economic losses induced by landslides. Theory and technics are available for worldwide application (Van Westen and Greiving., 2017;Huang et al., 2017;Lee et al., 2007;Neuhäuser and Terhorst, 2007;Van Westen et al., 2005;Erener et al., 2016;Jiménez-Perálvarez et al., 2017), but not yet well utilized in west Hubei, China, where the current research is undertaken. To date, very little scientific work is documented at the community level. Mountainous communities in this area are prone to landslide hazards, because of rainfall and the degree of urbanisation. Annually, road construction and anthropogenic modifications at the community scale (e.g., excavations in search of building material), the degree of urbanisation and subsequent population growth have accelerated more landslides of immense risk to the communities resulting in death and unaccountable losses in properties. According to the Chinese geological disaster notification report (2017), for example, around 850 disasters occurred in Hubei province, China, causing 23 deaths and about 254 million RMB (equal to ~ 38 million US Dollar, by May 2019 conversion) economic losses. It, therefore, remains a challenging problem to quantify landslide risk and develop reduction strategy.

Our objective in this work is to conduct a community-based landslide hazard probability and risk assessment on an area where limited landslide data and damage records exist. Despite these limitations, in this work, we will try; to quantify landslide risk for Yuyangguan community, Hubei province, China. The probabilistic method will be used to assess the landslide spatial, temporal and size probabilities. Landslide hazard and risk assessment will be considered for four return periods and two magnitude scenarios. Upon these, we expect to propose risk reduction strategies to the stakeholders in Yuyangguan town. This achievement may also be utilised into community scale landslide risk assessment in a mountainous area in Hubei, China.

2 Study area and data

The current study area, Yuyangguan community, is located in western Hubei province, China (Fig. 1). The study area was selected due to landslides that frequented this area and caused subsequent damages in recent years. It covers an area of about

https://doi.org/10.5194/nhess-2019-259
Preprint. Discussion started: 23 August 2019
© Author(s) 2019. CC BY 4.0 License.

Natural Hazards and Earth System Sciences
Discussions

34 km^2. The residential area is surrounded by steep slopes, with an elevation of 180 to 680 m.a.s.l. The climate is characterised as a typical monsoonal climate, with an average annual precipitation of about 1500 mm.

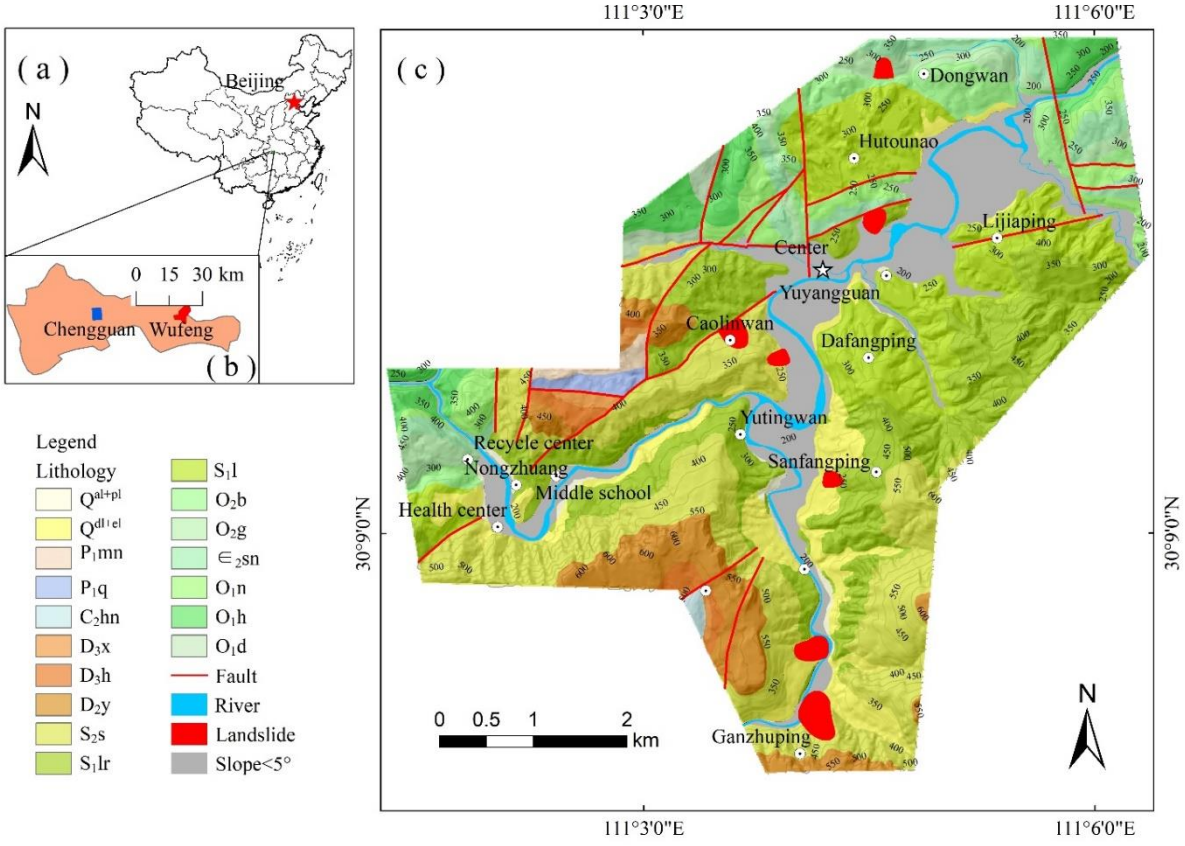

Fig. 1. a) Inset showing the map of China with the colour (b) representing the position of the current study area within China c) shows the main study area. (Lithology code is described in Table I)

The main lithological units outcropping in the study area comprise of Silurian sandstone and shale, Ordovician limestone with shale, Permian sandstone, Devonian with coal layer and recent deposits. Silurian sandstone is the dominant rock distributed along the community slopes. Intense weathering causes the bedrock to have low mass strength. Weathered rocks in Silurian are the primary source of landslides. Rainfall and human activities contribute significantly to the slope movement, mainly landslides. In the rainy season of 2013, a slope along the main road collapsed breaking and causing long traffic jam and transportation problems (Fig. 2). A landslide in the new residential quarter of the community occurred on the 3rd of January 2013. The foundation pit became unstable after one-day excavation (Fig. 3).

https://doi.org/10.5194/nhess-2019-259
Preprint. Discussion started: 23 August 2019
© Author(s) 2019. CC BY 4.0 License.

Natural Hazards and Earth System Sciences
Discussions

Table I. Characteristics of lithology distributed among Yuyangguan.

Lithology code	Characteristics of lithology
Q^{al+pl}	Gravel, pebble and drift stone, with a small amount of sand.
Q^{dl+el}	Clay intercalated with gravel, mainly distributing in the gentle slope area of bank slope.
P_1mn	The top marl, the middle thin layered manganese-bearing siliceous limestone.
P_1q	Upper Carboniferous Tumorous Limestone, Lower Chernite Nodules and Chernite Strip Limestone.
C_2hn	Upper thick layered limestone, dolomitic limestone, lower dolomite, sometimes conglomerate.
D_3x	Upper sandstone and shale interbedded, middle thick layered marl, lower sandy shale with oolitic hematite.
D_3h	Thin, medium-thick silty shale, fine-grained quartz sandstone, bottom shale.
D_2y	Thick quartzite and quartz sandstone with a small amount of carbonaceous shale and mudstone shale.
S_2s	Thick to thin layered quartz sandstone, siltstone and silty shale, mudstone shale at the lower part.
S_1lr	Shale with siltstone and thin marl.
S_1l	Muddy shale, sandy shale with siltstone, silty shale and carbonaceous shale.
O_2b	Medium-thick layered bioclastic turtle limestone.
O_2g	Microcrystalline limestone with a medium thickness.
O_1d	Thick to thin layers of tumorous limestone interbedded with shale.
O_1h	Thick and massive coarse-grained bioclastic limestone and limestone.
O_1n	Medium and thick layered limestone, dolomite and shale with limestone at the bottom.
$Є_2sn$	Massive and thick layered dolomite with dolomitic limestone.

https://doi.org/10.5194/nhess-2019-259
Preprint. Discussion started: 23 August 2019
© Author(s) 2019. CC BY 4.0 License.

Natural Hazards and Earth System Sciences
Discussions

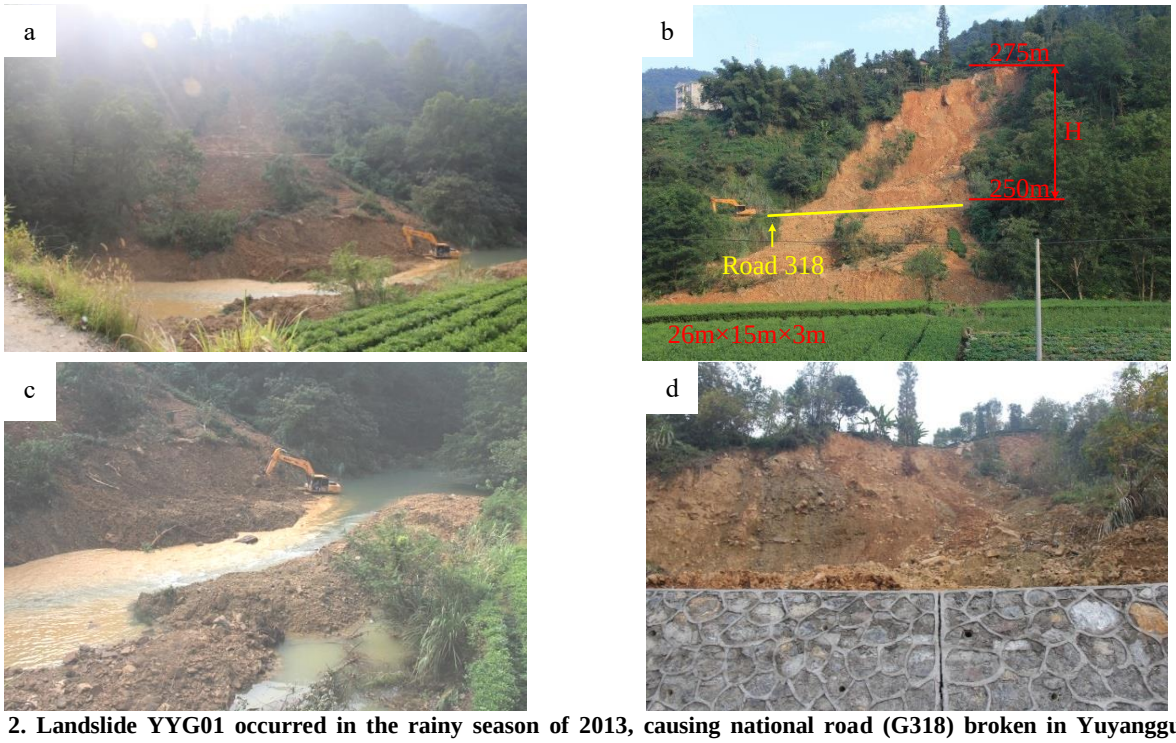

Fig. 2. Landslide YYG01 occurred in the rainy season of 2013, causing national road (G318) broken in Yuyangguan. (Travel distance=57m). a)An overview of landslide YYG01; b) Left side of landslide loose body; c) River blockage caused by landslide YYG01 and d) The retaining wall.

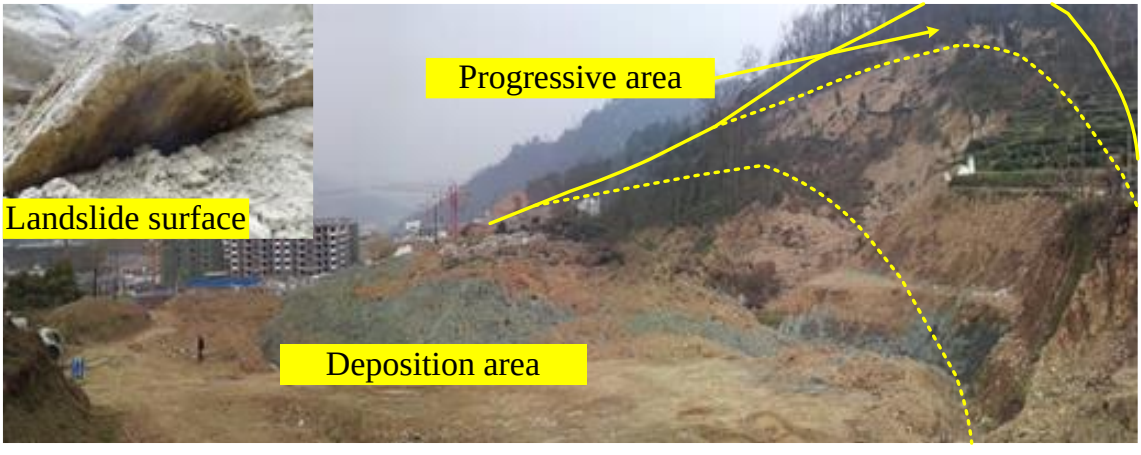

Fig. 3. Landslide YYG03 caused by slope cut in the residential quarter of Yuyangguan.

Landslide database is essential for landslide risk assessment. Seven landslides were interpreted from aerial photos, which were subsequently validated by the authors in the field. All the landslides mapped from 1976 to 2013 happened in areas where Quaternary deposit predominates. Besides the landslide inventory database, other datasets collected for landslide risk mapping include:

https://doi.org/10.5194/nhess-2019-259
Preprint. Discussion started: 23 August 2019
© Author(s) 2019. CC BY 4.0 License.

Natural Hazards and Earth System Sciences Discussions

- A 10m×10m resolution digital elevation model (DEM) generated from a topographic map obtained using an unmanned aerial vehicle (UAV). The DEM allowed the extraction of slope, elevation, aspect and curvature using the surface analysis tool available in ArcGIS (Fig. 4a, 4b, 4c, 4d).
- A Geological map at 1:50000 scale (Fig. 1) was used to extract datasets such as lithology, faults and slope structure map. The slope structure map (Fig. 4e) was generated using the standard and stratigraphic attitude advocated by Cruden (1991). Land use map was used to provide the distribution of rivers and roads (Fig. 4h, 4i).
- Due to a limited number of landslides (see Table II) data in Yuyangguan community, a landslide inventory database in Chengguan community was involved in this study to analyse the hazard probability. The location of Chengguan community is shown in Fig. 1b, which is in the same city and has a similar geological background with Yuyangguan (Fig. 1b).
- Building footprint map(Fig. 5) was interpreted and checked in the field by the authors. The majority of the buildings are located on or at the toe of the first slope zones with elevation up to 350 m.a.s.l. Entire build-up area is 18 610 000 m²; Data on the economic value of buildings was obtained from the department land and resource in Hubei province (See Table III).
- Census data was obtained by integrating the information derived from the China population data (2010) (http://www.stats.gov.cn/tjsj/pcsj/rkpc/6rp/indexch.htm) and sampling survey (Fig. 6). Total population is 45914 persons.

Table II. Historical landslides investigated in the field by the authors in Yuyangguan and Chengguan community.

Community	Landslide ID	Material	Bedrock	Volume(× 10 000 m³)	Area(× 10 000 m²)	Date (Year /month)	Triggering factors
Yuyangguan	YYG01	Soil	S_2s	147.6	5.9	2013.7	R
	YYG02	Soil	S_1lr	49.8	4	1981.6	R & SC
	YYG03	Soil	S_1l	20.9	1.7	2014.1	R & SC
	YYG04	Soil	S_2s	10.7	1.5	2013.5	R & SC
	YYG05	Soil	S_2s	10.4	3.5	1989.1	R
	YYG06	Soil&rock	O_2g	8	1.6	2007.12	R & SC
	YYG07	Rock	O_2g	22.2	2.2	2010.6	R & SC
Chengguan	CG01	Soil	S_1l	5.4	0.45	2009.5	R

https://doi.org/10.5194/nhess-2019-259
Preprint. Discussion started: 23 August 2019
© Author(s) 2019. CC BY 4.0 License.

Natural Hazards and Earth System Sciences
Discussions

CG02	Soil	S_1l	1.05	0.21	2012.4	R
CG03	Rock	O_2b	1.92	0.48	1991.7	R
CG04	Rock	O_2b	5.04	0.56	2005.8	SC
CG05	Soil	O_2b	55.9	4.3	2002.7	R & SC
CG06	Rock	O_2b	34.5	2.3	1992.6	R
CG07	Soil	O_2b	14.3	1.1	1997.7	R
CG08	Soil	O_2b	79.5	5.3	1967.6	R
CG09	Soil&rock	O_2b	16.8	2.4	1969.7	R
CG10	Soil	O_2b	3.18	0.53	2012.3	R
CG11	Soil	S_1l	7	0.5	1992.6	R
CG12	Soil	S_1l	9.6	1.2	1992.6	R
CG13	Soil	S_1l	4.55	0.65	1994.7	R
CG14	Soil	S_1l	8.2	0.82	1994.7	R
CG15	Soil	S_1l	8	0.8	1998.2	R
CG16	Soil	S_1l	3.6	0.6	1996.7	R
CG17	Soil	S_1l	4	0.5	1969.7	R
CG18	Soil	S_1l	13.2	1.1	2007.7	R
CG19	Soil	S_1l	4.32	0.54	1991.6	R

R-rainfall； SC- Slope cut. The code of Bedrock is listed in Table I.

95

https://doi.org/10.5194/nhess-2019-259
Preprint. Discussion started: 23 August 2019
© Author(s) 2019. CC BY 4.0 License.

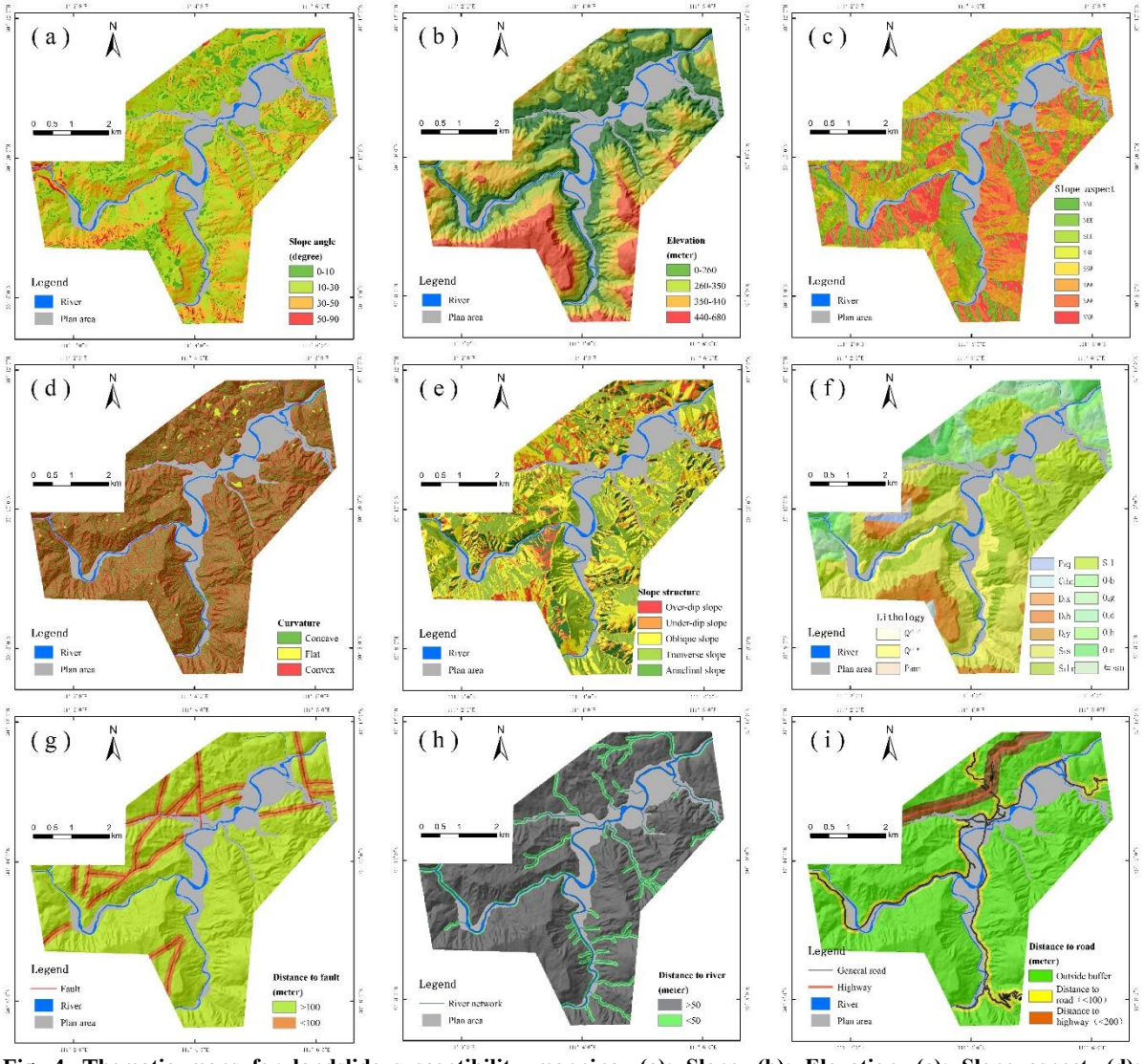

Fig. 4. Thematic maps for landslide susceptibility mapping. (a): Slope, (b): Elevation, (c): Slope aspect, (d): Curvature, (e): Slope structure, (f): Lithology, (g): Distance to fault, (h): Distance to river, (i): Distance to road.

https://doi.org/10.5194/nhess-2019-259
Preprint. Discussion started: 23 August 2019
© Author(s) 2019. CC BY 4.0 License.

Natural Hazards and Earth System Sciences
Discussions

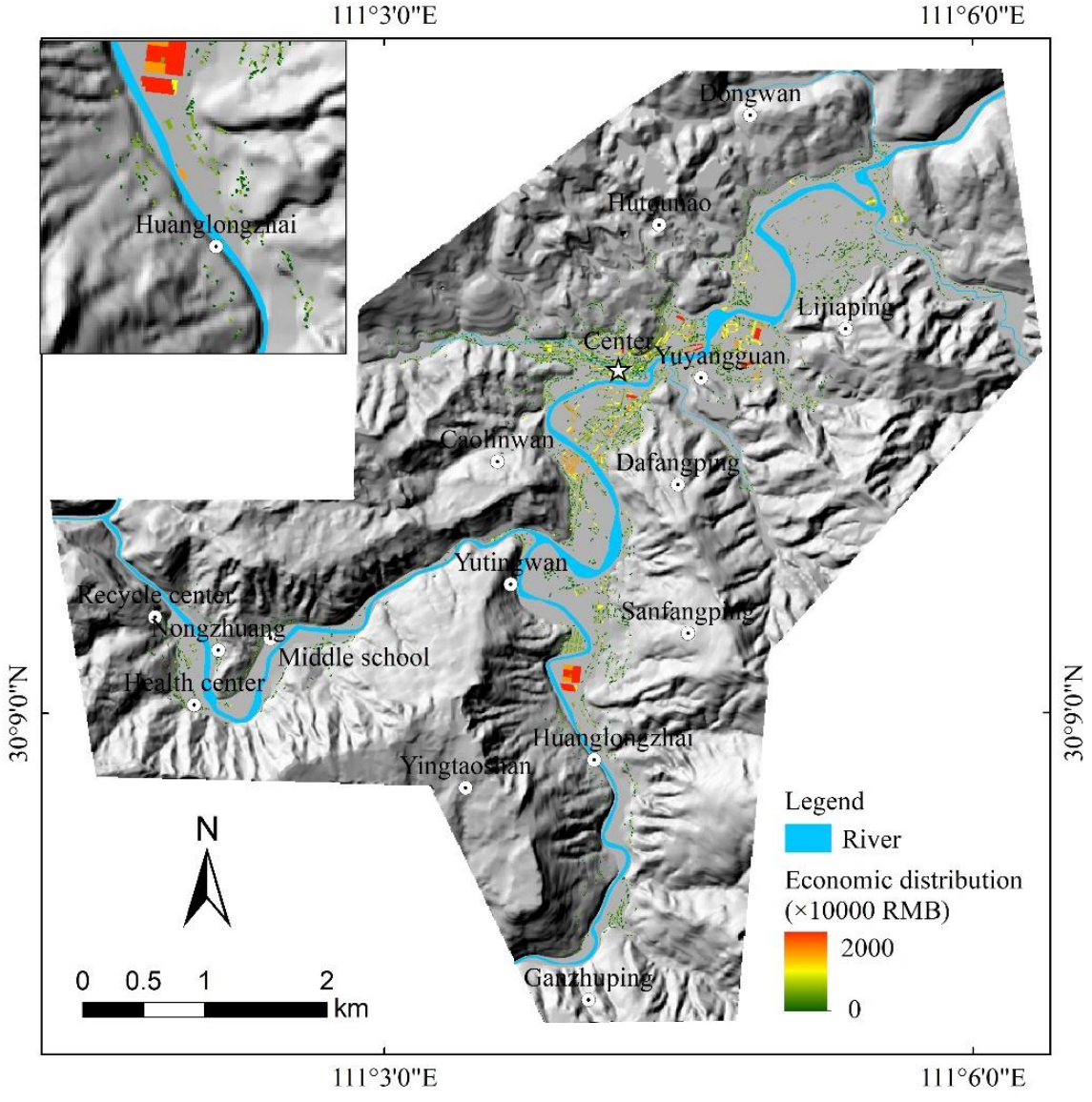

Fig. 5. Building footprint map with economic values.

Table III. The economic value of buildings in Yuyangguan community (the department land and resource in Hubei province, 2016).

Typology	1 000 RMB/ m^2	Numbers of floor
Reinforced	3.12	20-32
Reinforced concrete	1.33	6-20
Masonry	0.8	2-6
Wooden	0.1	1-2

https://doi.org/10.5194/nhess-2019-259
Preprint. Discussion started: 23 August 2019
© Author(s) 2019. CC BY 4.0 License.

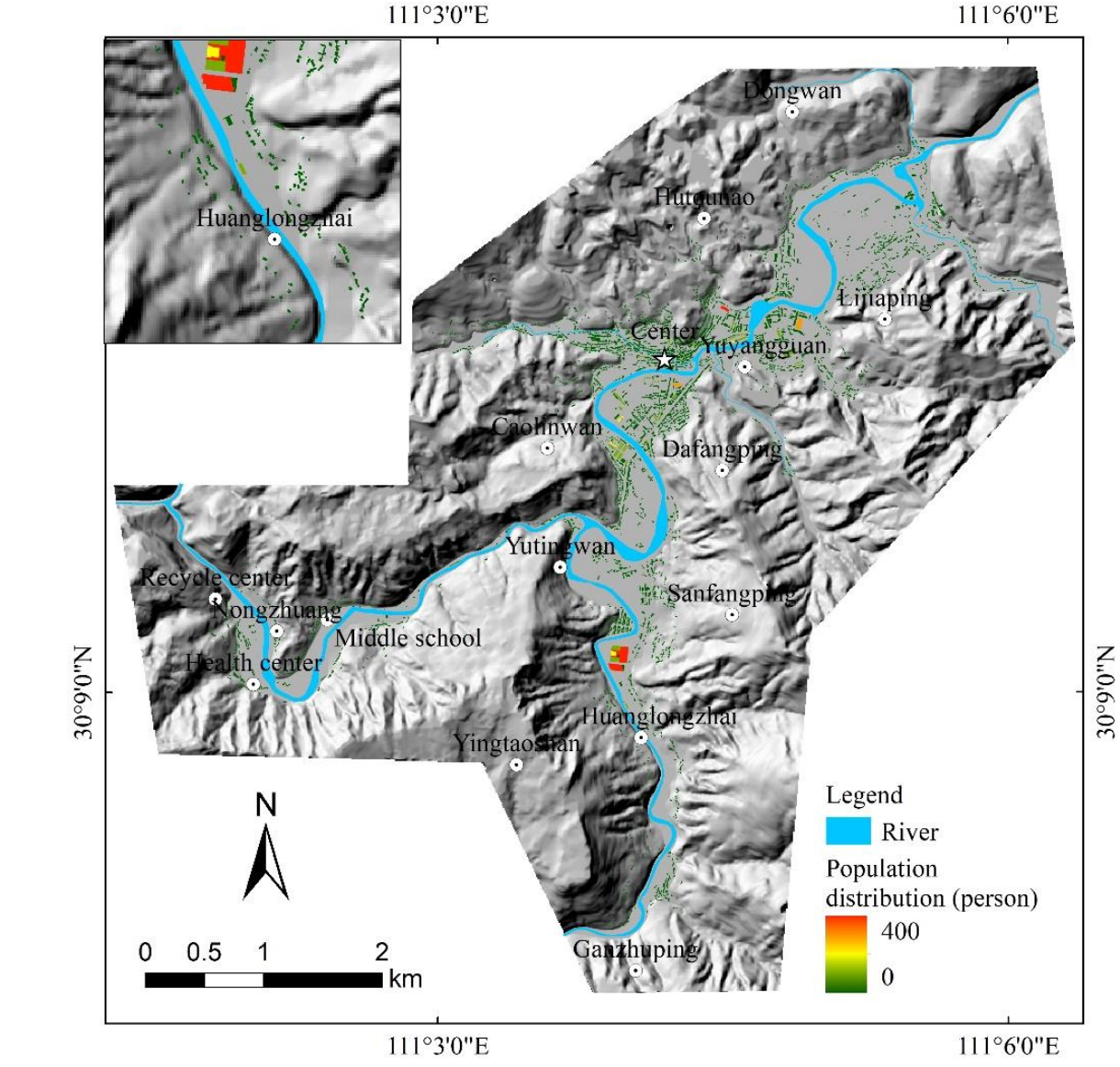

Fig. 6. Population distribution map of Yuyangguan community.

3 Methodology

This section explains the method used to conduct a semiquantitative risk analysis for landslides at a community scale. As a start, the slope unit based hazard probability was calculated by integrating spatial, temporal and size probabilities. We
105 generated eight hazard probability maps, considering four return periods (5, 10, 20 and 50 years) and two size scenarios. For each map, we determined the landslide potential influencing area semiquantitatively by calculating the travelling distance of

https://doi.org/10.5194/nhess-2019-259
Preprint. Discussion started: 23 August 2019
© Author(s) 2019. CC BY 4.0 License.

Natural Hazards and Earth System Sciences Discussions

the slope unit. Subsequently, the element-at-risk map and the vulnerability map were created by assimilating assets and landslide influencing area. The combination of hazard maps with vulnerability and element-at-risk leads to the risk value for each slope unit, which contributes to the final risk maps in the study area.

3.1 Landslide hazard from spatial, temporal and size probability analysis

Hazard assessment is an essential step in landslide risk assessment. For the community scale, this can be achieved by applying the deterministic model (Qiao et al., 2019;Gokceoglu and Aksoy, 1996) if detailed engineering geology data is enough. For the study area, soil or rock strength parameters are not available if using the deterministic method. However, we can use three probabilities (spatial, temporal and size) to answer the question of where and how potential landslides will occur with absolute magnitude in a given time ((Guzzetti et al., 2005).

$$H = P(S) \times P(N_L) \times P(A_L) \quad (1)$$

Where H represents hazard probability; $P(S)$ is spatial probability; $P(N_L)$ is a temporal probability, and $P(A_L)$ is size probability.

Spatial probability, based on the concept of susceptibility, assesses the locations where a mass movement exists or may potentially occur. Landslide susceptibility mapping (LSM) is now widely used by various researchers (Guzzetti et al., 2012;Fell et al., 2008b;Ayalew et al., 2004;Van Westen et al., 2008). In this paper, morphometric and geo-environmental factors were chosen as variables. These include altitude, slope, aspect, curvature, slope structure, distance to rivers, and proximity to roads. These Morphometric factor maps were derived from the digital elevation model (DEM), with resolution 10×10 m obtained by Unmanned Aerial Vehicle (UAV). Geo-environmental factors such as lithology and faults were prepared and transformed from shapefile to grid-based map, using the 1:10 000 scaled geological field map obtained from Bureau of China Geological Survey (http://www.cgs.gov.cn/). The detailed processing steps in ArcGIS are explained in the paper of Catani, Casagli, Ermini, Righini, & Menduni (2005). The most common and widely applied weight of evidence (WoE) method was used to assess landslide susceptibility in this paper. It is a probabilistic model considering evidence factors of landslides, based on conditional independence hypothesis (Hong et al., 2017). In WoE method, the contrast (difference of W^+ and W^-) was used as a weight for each morphometric or geo-environmental factor. The effectiveness of LSM was tested using the Receiver Operating Characteristics (ROC) curve (Metz, 1978;Zezere et al., 2017). The area under the ROC curve is used to assess the success rate.

The above grid-based LSM was then converted into a slope unit based susceptibility map. Susceptibility value in each slope was calculated from the average value of susceptibility of the grids inside the slope. The slope unit was subdivided using the hydrology analysis method in ESRI ArcGIS platform (http://www.esri.com/software/arcgis/arcgisonline). The slope unit based spatial probability map was classified into five classes: very high, high, moderate, low, and very low.

https://doi.org/10.5194/nhess-2019-259
Preprint. Discussion started: 23 August 2019
© Author(s) 2019. CC BY 4.0 License.

Natural Hazards and Earth System Sciences Discussions

Landslide temporal probability $P(N_L)$ is evaluated based on the assumption that slope failures can be viewed as independent random points-event in the time dimension (Crovelli, 2000;Guzzetti et al., 2006). In this study, the Poisson model (Crovelli, 2000) was adopted to construct temporal probability. It is here an exceedance probability of landslide occurrence during a given period (see equation (2), which means the probability of experiencing one or more landslides during a given time.

$$P(N_L) = 1 - e^{-T/RI}, RI = t / N \quad (2)$$

Where, *T* is the return period, e.g. 1, 10, 20 and 50 years; *RI* is the historical mean recurrence interval for each slope unit; *t* is the temporal interval of landslide database, and *N* is the number of landslides recorded in each slope. If incomplete historical landslide database exists, the value of *N* on the slope units with very high susceptibility class in LSM is assigned as 1.

Landslide size probability is calculated based on the relationships between landslide volume and cumulative frequency. Guzzetti et al. (2005) used the probability density function of the landslide area to predict the probability of one specific landslide area in each slope unit. Stark and Hovius (2001) found that landslides in New Zealand and Taiwan fitted with a double Pareto probability distribution. Two differences in our study will improve the application. The first one is that the present research is to find the most suitable distribution for the case study area. Therefore, we compared the above distributions and tried other type using Ordinary Least Square (OLS) method in Matlab software. The best-fitted one was then used for probability calculation. The second one is that landslide volume is an acceptable indicator for risk control practice in the study area. Therefore, we converted the landslide size probability distribution from area to volume in this paper, using the volume-area relationship simulated by the OLS method. For this, we used the historical landslides in the database from the study area and the Chengguan community in Table II. Meanwhile, two size scenarios were determined from the distribution of landslides volume in the case study area.

3.2 Data preparation for elements- at- risk

The next step is to determine the elements at landslide risk. This study focuses on residential buildings and people inside these buildings. The building footprint map (see Fig. 5) was interpreted from the image data of UAV in 2013. Building structure (reinforced, reinforced concrete, masonry, wooden) and numbers of floors are involved in the building map database. To express the risk in monetary values, we used the economic value of buildings (see Table III) obtained from the Department of Hubei Province Land and Resource. This data was converted to building values by multiplying unit economic values, footprint area and the number of floors. Data of population inside buildings were obtained by integrating the information from China population census data (2010) and sampling survey. The average number of people per building was calculated by applying a Dasymetric Mapping Approach (a methodology for generating a surface-based representation of the population) (Mennis, 2003), which contributes to the data of the population inside each building. In order to assess the element-at-risk, the building footprint map was then intersected with the potential landslide influence area at the community

https://doi.org/10.5194/nhess-2019-259
Preprint. Discussion started: 23 August 2019
© Author(s) 2019. CC BY 4.0 License.

Natural Hazards and Earth System Sciences Discussions

level. The influence area of each slope was semiquantitatively determined by calculating the travel distances by the following formula (Hungr et al., 2005).

$$log(H/L) = A + B \times logV \quad (3)$$

Where L is travel distance; H is slope height; V is slope volume; A and B are constants, referred from Corominas (1996).

3.3 Vulnerability analysis and risk assessment

Quantitative vulnerability analysis is still a challenge in landslide risk assessment(Peduto et al., 2017;Chen et al., 2011). Physical vulnerability assessment can be performed in large or local scale area (Quan Luna et al., 2011;Li et al., 2010;Fell et al., 2008b). In this study, the physical vulnerability was semiquantitatively determined for buildings using two indicators. The first indicator relates to building structures such as reinforced, reinforced concrete, masonry and wooden. The second indicator is the landslide travel distance. The assumption is that vulnerability is 1.0 for the buildings on the slope, and decreases from the toe of surface rupture to the farthest travel distance. We proposed a set of vulnerability value for buildings with different types (see Table IV).

Table I. Vulnerability value of buildings impacted by landslides (proposed by authors)

	Influence area			
	Zone 1	Zone 2	Zone 3	Zone 4
Reinforced	0.1	0.3	0.5	1
Reinforced concrete	0.2	0.5	0.7	1
Masonry	0.3	0.7	0.9	1
Wooden	0.4	0.9	1	1

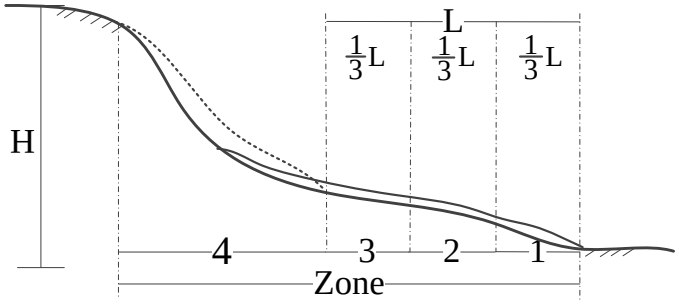

(L is travel distance; H is slope height)

The vulnerability of the population inside the buildings follows a power-law relationship with building vulnerability (Li et al., 2010), as follows (see equation (4)):

$$V_p = 0.0014 \times e^{6.07 \times V_b} \quad (4)$$

Where V_p is the vulnerability of population inside buildings; V_b is the vulnerability of buildings.

Landslide risk map was then generated in ArcGIS based on the concept defined by IAEG and Varnes (1984) as "the expected number of lives lost, persons injured, damage to property and disruption of economic activity due to a particularly damaging phenomenon for a given area and reference period". The conceptual equation of risk is:

$$R = H \times V \times E \quad (5)$$

https://doi.org/10.5194/nhess-2019-259
Preprint. Discussion started: 23 August 2019
© Author(s) 2019. CC BY 4.0 License.

Natural Hazards and Earth System Sciences Discussions

Where *R* is the expected losses in some return periods; *H* is the landslide probability in some return period with a given size scenario. In the present study, *V* is the physical vulnerability of buildings or populations inside buildings. *E* is the quantification of the exposed elements at risk. Using Equation 5, the risk curve can be fitted by plotting the probability versus potential loss and the annual risk can then be calculated using the area under the risk curve (van Westen, 2002)

4 Results

This section provides the results of the case study to illustrate the application of proposed framework and methodology in Section 3.

4.1 Landslide susceptibility assessment

In assessing landslide susceptibility, we have looked into the elevation, slope, aspect, curvature, lithology, slope structure, distance to fault, rivers and roads. The weight and contrast value by WoE method for LSM of Yuyangguan is shown in Table V. As can be seen in this Table, the contrast values explained in section 3.1 for lithology shows that the O_2g and Q_4^{dl+el} are the top two units. This implies that these two lithological units can be susceptible to erosion and can quickly accelerate erosion and loss of stability thus triggering landslides.

General road construction contributes secondary importance, with the contrast value of 0.95. Table V also indicates that the morphometric factor in the study area is generally significant. In the case of aspect and elevation, the contrast value was high on the north facing slopes with elevation from 0 to 260 m.a.s.l, but low on the south-facing slopes with elevation above 350 m.a.s.l. In the case of the slope, the steeper the slope is, the higher the landslide probability. The value of slope varies from 10°to 30°is 0.19, which indicates a relatively high landslide probability.

The grid-based susceptibility map was converted to a slope unit based map with 701 slope units in total. As shown in Fig. 7, the slope unit based susceptibility map was ordered into five classes ranging from very low to very high. The performance of this map shows an accuracy of 84% using the ROC curve. The landslide susceptibility in this study area is very high on the north-facing slopes along the main road, especially where Q_4^{dl+el} and O_2g rocks are present. These results correspond well with the contrast value shown in Table V.

https://doi.org/10.5194/nhess-2019-259
Preprint. Discussion started: 23 August 2019
© Author(s) 2019. CC BY 4.0 License.

Natural Hazards and Earth System Sciences Discussions

Table V.The weight and contrast value by Weight of Evidence model for landslide susceptibility mapping of Yuyangguan, west Hubei, China

Factors	Classes	Area of domain %	Landslide area %	W^+	W^-	$C=W^+-W^-$	$S^2(W^+)$[a]	$S^2(W^-)$[b]	S(C)[c]	C/S (C) [d]
Slope	0--10	11.03	3.66	-1.11	0.08	-1.19	0.01	0.00	11.04	-13.15
(degrees)	10--30	55.76	67.48	0.19	-0.31	0.5	0.00	0.00	27.44	13.84
	30--50	30.77	28.86	-0.07	0.03	-0.09	0.00	0.00	26.53	-2.45
	50--90	2.44	0	0	0.02	-0.02	-	0.00	-	-
Elevation	0--260	30.99	51.21	0.51	-0.35	0.86	0.00	0.00	29.24	25.15
(meters)	260--350	35.75	43.11	0.19	-0.12	0.31	0.00	0.00	28.99	9.07
	350--440	19.81	5.68	-1.26	0.16	-1.42	0.01	0.00	13.60	-19.36
	440--680	13.44	0	0	0.15	-0.15	-	0.00	-	-
Aspect	Plan area	2.32	0.14	-2.79	0.02	-2.81	0.20	0.00	2.23	-6.29
(degrees)	NNE(0～45°)	12.08	10.06	-0.19	0.02	-0.21	0.00	0.00	17.63	0.00
	NEE(45～90°)	10.86	17.23	0.47	-0.08	0.54	0.00	0.00	22.05	12.00
	SEE(90～135°)	11.48	7.06	-0.49	0.05	-0.54	0.00	0.00	15.03	-8.11
	SSE(135～180°)	12.51	7.44	-0.52	0.06	-0.58	0.00	0.00	15.40	-8.96
	SSW(180～225°)	12.25	7.2	-0.54	0.06	-0.59	0.00	0.00	15.17	-8.99
	SWW(225～270°)	12.16	5.88	-0.73	0.07	-0.8	0.00	0.00	13.81	-11.09
	NWW(270～315°)	12.18	15.59	0.25	-0.04	0.29	0.00	0.00	21.21	6.17
	NNW(315～360°)	14.17	29.39	0.74	-0.2	0.94	0.00	0.00	26.56	24.97
Lithology	Q^{al+pl}	0.78	0.06	-2.61	0.01	-2.62	0.50	0.00	1.41	-3.70
	Q^{dl+el}	8.08	50.95	1.91	-0.63	2.54	0.00	0.00	28.83	73.28
	P_1mn	0.58	0	0	0.01	-0.01	-	0.00	-	-
	P_1q	0.75	0	0	0.01	-0.01	-	0.00	-	-
	C_2hn	0.26	0	0	0	0	-	0.00	-	-
	D_3x	0.63	0	0	0.01	-0.01	-	0.00	-	-
	D_3h	1.24	0	0	0.01	-0.01	-	0.00	-	-
	D_2y	7.16	0	0	0.08	-0.08	-	0.00	-	-
	S_2s	22.07	27.61	0.23	-0.07	0.3	0.00	0.00	26.15	7.88
	S_1lr	21.34	11.99	-	0.11	-0.7	0.00	0.00	19.06	-13.26

https://doi.org/10.5194/nhess-2019-259
Preprint. Discussion started: 23 August 2019
© Author(s) 2019. CC BY 4.0 License.

Natural Hazards and Earth System Sciences
Discussions

				0.58						
	S_1l	15.18	0	0	0.17	-0.17	-	0.00	-	-
	O_2b	4.54	0	0	0.05	-0.05	-	0.00	-	-
	O_2g	3.33	9.37	1.06	-0.07	1.12	0.00	0.00	16.89	18.94
	O_1d	3.83	0.03	-4.9	0.04	-4.94	1.00	0.00	1.00	-4.94
	O_1h	4.71	0	0	0.05	-0.05	-	0.00	-	-
	O_1n	4.69	0	0	0.05	-0.05	-	0.00	-	-
	$Є_2sn$	0.84	0	0	0.01	-0.01	-	0.00	-	-
Curvature	Concave	48.71	51.94	0.07	-0.07	0.14	0.00	0.00	29.25	4.11
	Stright/flat	0.87	0.03	-3.42	0.01	-3.43	1.00	0.00	1.00	-3.43
	Convex	50.42	48.03	-0.05	0.04	-0.09	0.00	0.00	29.26	-2.54
Slope	Over-dip	9.88	12.28	0.22	-0.03	0.25	0.00	0.00	19.19	4.78
structure	Under-dip	5.8	2.39	-0.89	0.04	-0.93	0.01	0.00	8.98	-8.32
	Obique	15.19	6.71	-0.82	0.1	-0.92	0.00	0.00	14.70	-13.49
	Tranverse	32.32	33.29	0.03	-0.02	0.05	0.00	0.00	27.59	0.00
	Anaclinal	36.82	45.33	0.21	-0.15	0.36	0.00	0.00	29.14	10.47
Distance to fault	>100	84.96	88.47	0.04	-0.27	0.31	0.00	0.00	18.72	5.80
(meters)	<100	15.04	11.53	-0.27	0.04	-0.31	0.00	0.00	18.72	-5.80
Distance to rivers	>50	89.57	87.26	-0.03	0.2	-0.23	0.00	0.00	19.50	-4.46
(meters)	<50	10.43	12.74	0.2	-0.03	0.23	0.00	0.00	19.50	4.46
Distance to	Outside buffer	83.76	69.63	-0.19	0.64	-0.82	0.00	0.00	26.84	-22.09
road	General road(<100)	9.73	21.59	0.81	-0.14	0.95	0.00	0.00	23.95	22.85
(meters)	Highroad(<200)	6.52	8.79	0.3	-0.02	0.33	0.00	0.00	16.55	5.44

The total area of the community are is 29.14 square kilometers.

Total landslide area is 3740 pixels.

[a]Variance of W^+

[b]Variance of W^-

[c]Standard deviation of contrast

[d]Studentized value of contrast

https://doi.org/10.5194/nhess-2019-259
Preprint. Discussion started: 23 August 2019
© Author(s) 2019. CC BY 4.0 License.

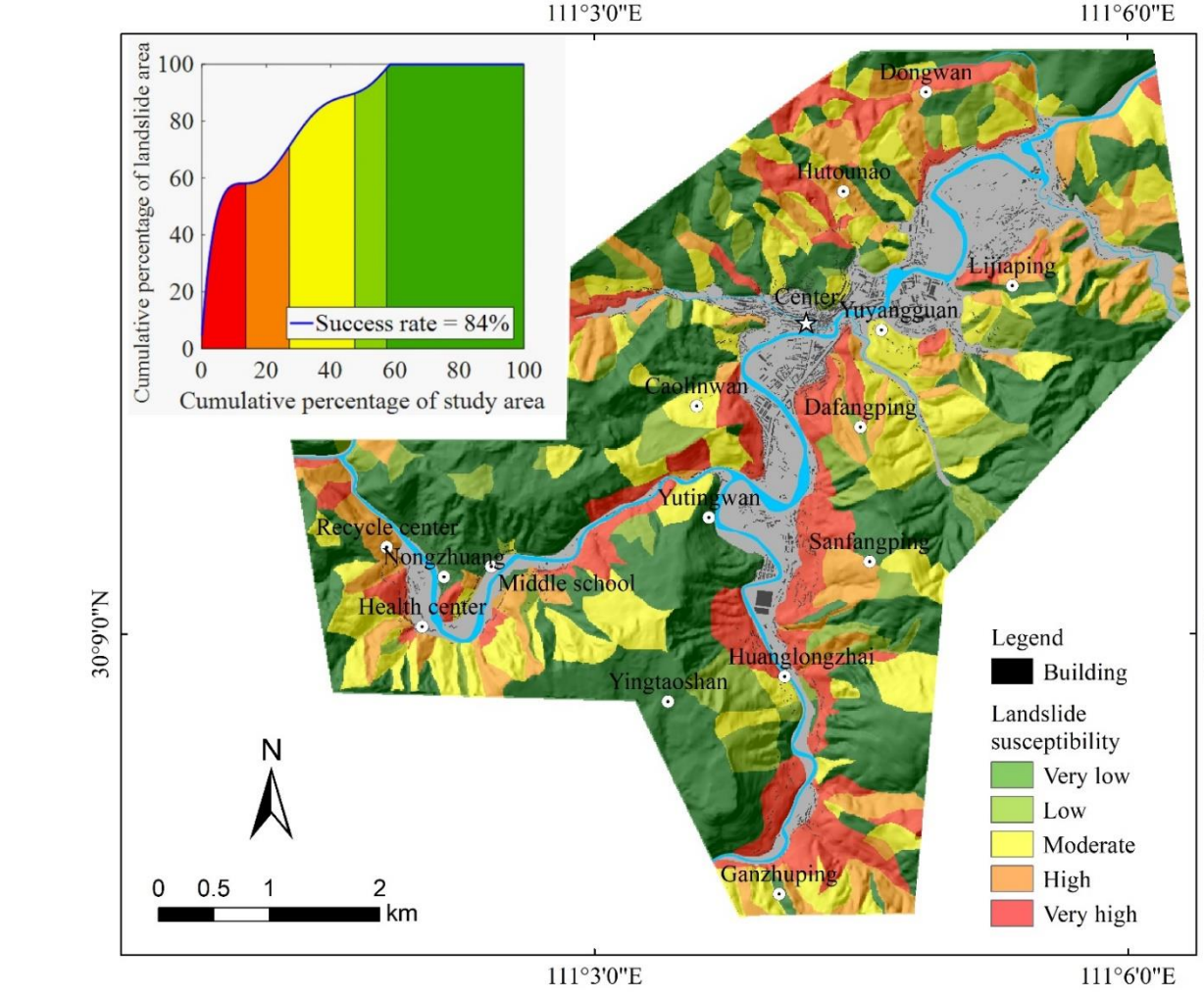

Fig. 7. Slope unit based landslide susceptibility map (LSM) at the community level, converted from the grid-based LSM using the weight of evidence method for Yuyangguan, west Hubei, China

4.2 Landslide hazard probability

Landslide hazard involves spatial, temporal and size probabilities. The landslide database of Yuyangguan shown in Table II, covers the temporal interval of 33 years starting from 1981 to 2013. For each slope unit, the historical mean recurrence interval (*RI)* was calculated using Equation 2. Assuming that the past is the future, landslides in the study area will probably occur with the same amount of landslides over the next 50 years as the past 50 years.

Fig. 8 shows four landslide temporal probability maps for four return periods (5, 10, 20, 50 years). The map for 50 years, for example, indicates the probability of the slope units experiencing landslide events is the highest among the four maps. Slope units with high and very high probability value (greater than 0.5) mostly cluster on the first slope zones around the

https://doi.org/10.5194/nhess-2019-259
Preprint. Discussion started: 23 August 2019
© Author(s) 2019. CC BY 4.0 License.

Natural Hazards and Earth System Sciences
Discussions

community. The probability value on these slopes increases from the return period of 5 years. For example, Enlarged window in maps of Fig. 8 shows that the slope in Huanglongzhai village experienced a very low probability in 5-year to a high class in a 50-year return period.

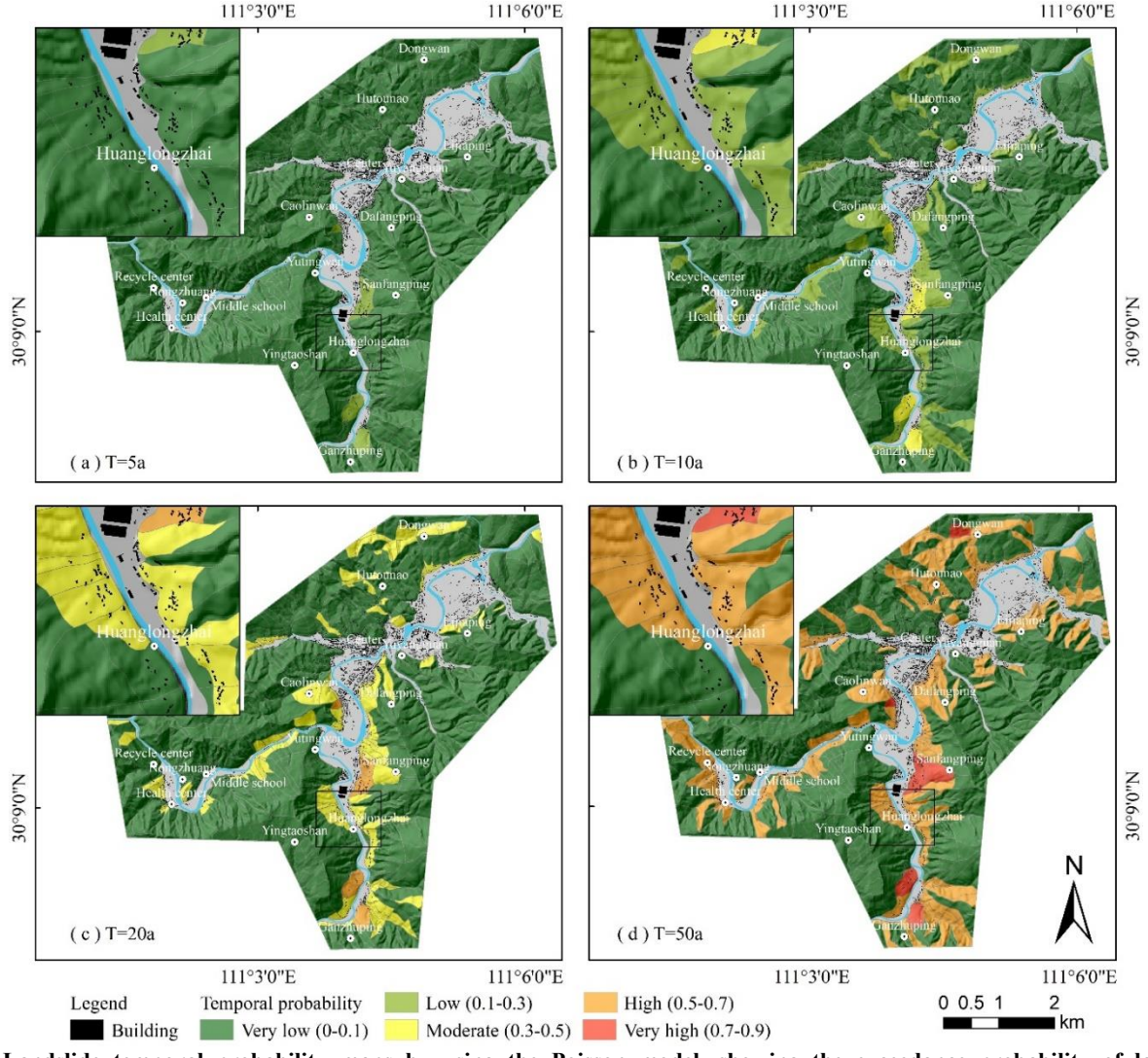

Fig. 8. Landslide temporal probability maps by using the Poisson model, showing the exceedance probability of landslide occurrence in each slope unit during four return periods (5, 10, 20, 50 years).

The landslide probability distribution curves are created using three different fitting functions, shown in Fig. 9. In comparison to the inverse gamma and the power law distributions, the function by OLS method shows the best fitting degree, with the smallest root mean square error (RMSE) of 0.05. This indicates that landslide frequency distribution function by the OLS method is the most appropriate technique to apply in Yuyangguan. The volume-area relationship is analysed in Fig. 10a with R-square 0.915. This indicates that the way of converting size probability distribution from landslide area data to

https://doi.org/10.5194/nhess-2019-259
Preprint. Discussion started: 23 August 2019
© Author(s) 2019. CC BY 4.0 License.

Natural Hazards and Earth System Sciences
Discussions

volume is feasible in the study area. Meanwhile, two size scenarios are determined from the cumulative frequency curve in Fig. 10b in terms of landslide volume: 50 000 cubic meters and 100 000 cubic meters.

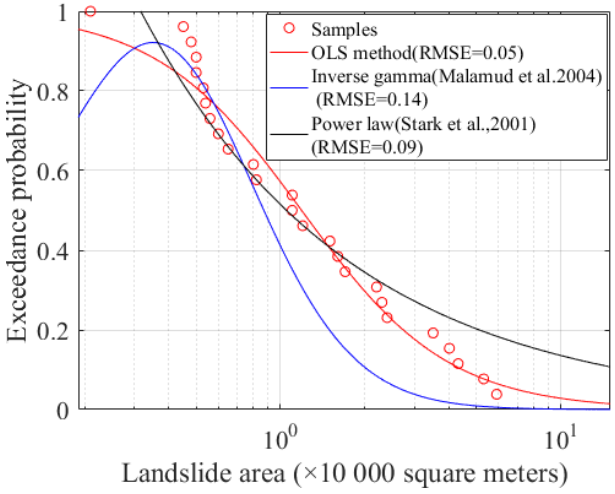

OLS method: $$p=\frac{1}{1+a_1 A_L^{2a_2}}$$

Inverse gamma:

$$p(A_L;\rho,a,s)=\frac{1}{a\Gamma(\rho)}\left[\frac{a}{A_L-s}\right]^{\rho+1} * \exp\left[-\frac{a}{A_L-s}\right]$$

Power law: $$p=a_3 A_L^{-a_4}$$

Where, p is probability; A_L is landslide area; a=1.89, a_1=0.75, a_2=0.83, a_3=0.51, a_4=0.58; ρ=2.42, s=-0.20

Fig. 9. Magnitude-frequency relationships simulated by Ordinary Least Square method, Inverse gamma, and Power law for landslide in western Hubei. Samples are from Table II, which involves the Chengguan database except for the study area.

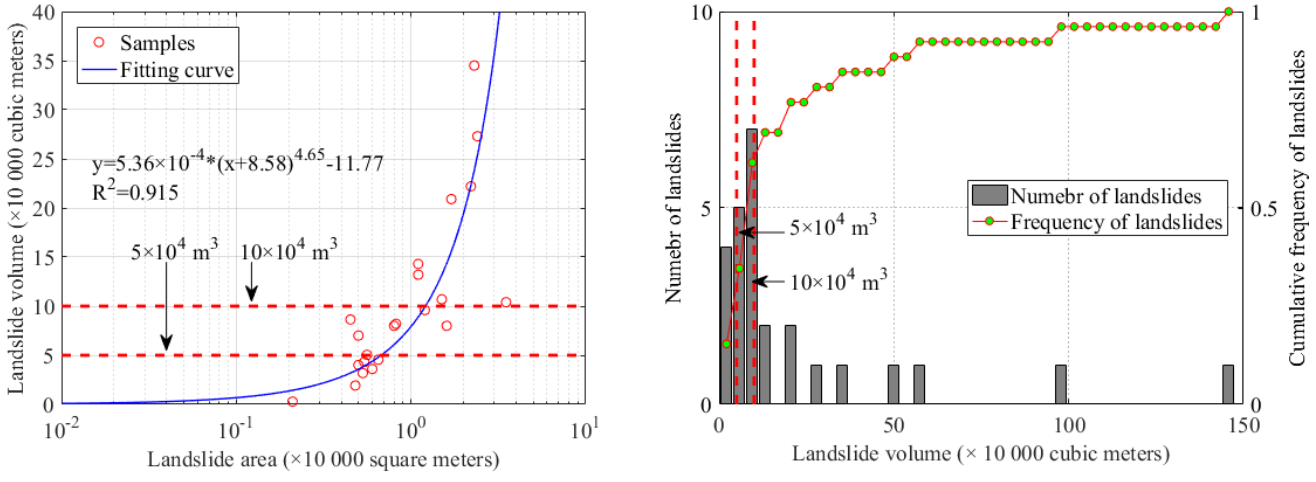

Fig. 10. (a) Relationship of landslide volume and area (R^2=0.915), which will be used to convert magnitude-frequency relationships in terms of area to landslide volume. (b) Frequency distribution of Landslide volume. Samples are from Table II, which involves Chengguan database except for the study area.

https://doi.org/10.5194/nhess-2019-259
Preprint. Discussion started: 23 August 2019
© Author(s) 2019. CC BY 4.0 License.

Natural Hazards and Earth System Sciences
Discussions

Integrating the spatial probability in Fig. 7, temporal probability in Fig. 8 and the magnitude-frequency relationships in Fig. 9 by using Equation 1, we then obtain eight hazard maps. In these maps, we demonstrate the hazard probability for each slope unit for four return periods (5, 10, 20, 50 years) and two different landslide sizes equal or greater than 50 000 m³, and
235 equal or greater than 100 000 m³. As an example, Fig. 11 shows the four landslide hazard maps for four return periods and the landslide sizes scenario equal to or greater than 50 000 m³. In these maps, landslide hazard probability values were classified into five categories from very low (0.0-0.1) to very high (0.4-0.5). The map for 50 years returns period shows that most building areas of the community located at the bottom or near the slopes with very high hazard probabilities. Additionally, buildings located in the community centre are in low to very low hazard probability areas.

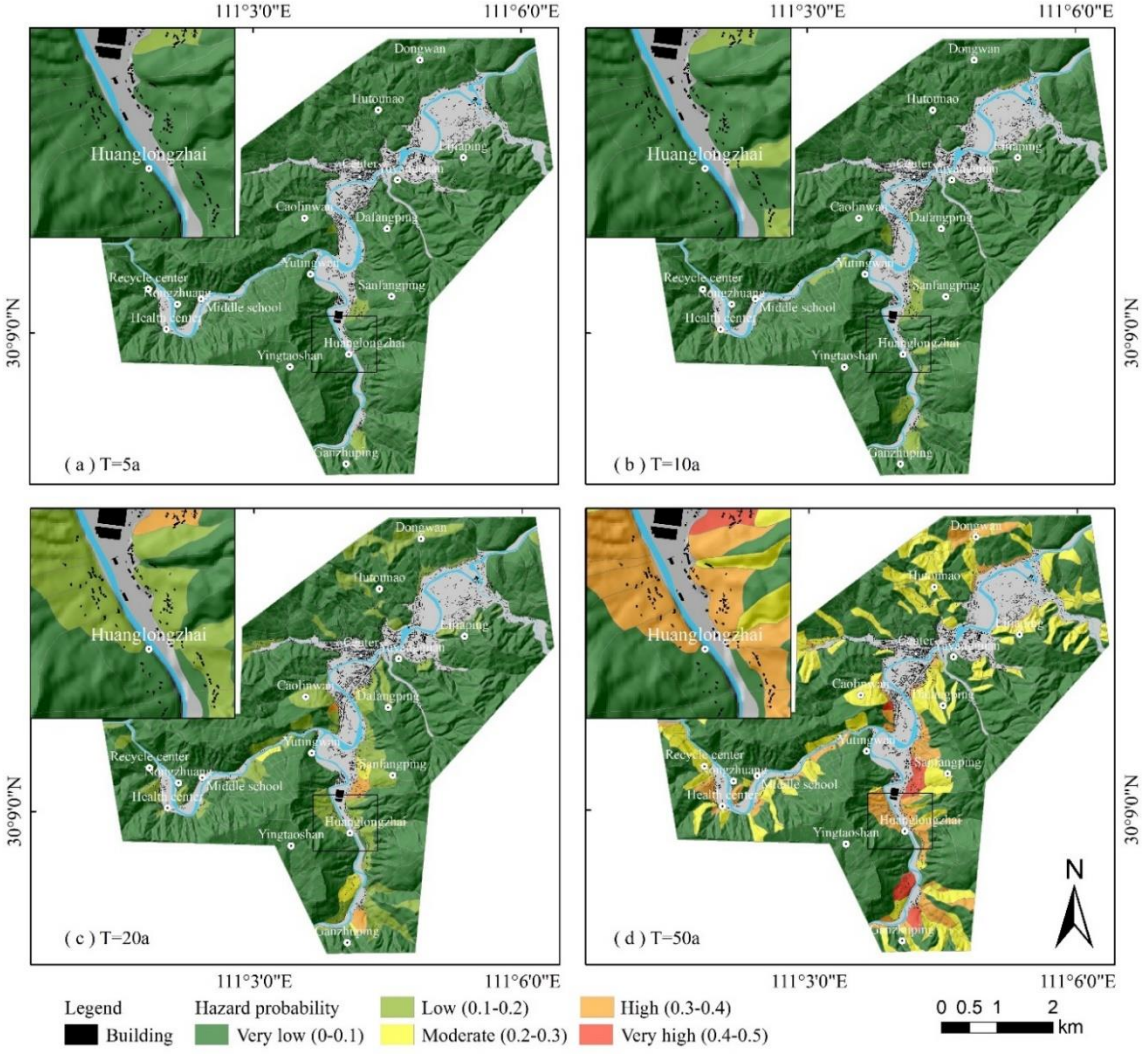

Fig. 11. The Landslide hazard maps for four return periods (5,10,20,50 years) and the landslide sizes scenario equal to or greater than 50 000 m³. The maps were generated by integrating the spatial probability in Fig. 7, temporal probability in Fig. 8 and the magnitude-frequency relationships in Fig. 9.

https://doi.org/10.5194/nhess-2019-259
Preprint. Discussion started: 23 August 2019
© Author(s) 2019. CC BY 4.0 License.

Natural Hazards and Earth System Sciences Discussions

4.3 Element-at-risk and vulnerability assessment

We assume that the buildings and population inside the buildings are exposed to the slopes with high and very high-class probability in hazard maps. Therefore, the element-at-risk maps for buildings and population generated from the data in Section 2 and methodology in Section 3.2 are consistent with the four return periods and two size scenarios of landslide hazard probability maps.

Table VI shows that in the return periods of five years and ten years, there is no exposure, while in the case of 50 years return period and 50 000 m^3 size scenario there are 570 000 m^2 build-up areas and 14 257 persons identified to be exposed to landslide risk. The table also indicates the tendency of potentially damaged building areas and the number of persons within the buildings from the return period of 20 years to 50 years. The vulnerability value was indirectly calculated by equation 4 in Section 3.3. In the size scenario of landslide, volume equal to or greater than 50 000 m^3, a sharp increase of exposure exists both for built-up areas and populations. The exposure over doubled from 20 years to 50 years. This result also exits for the size scenario of landslide volume equal to or greater than 100 000 m^3. Comparing the two different size scenarios, we find that the number of exposure of 100 000 m^3 volume is smaller than that of 50 000 m^3. There are 8.76 per cent building areas exposed to landslide in 20 years return period. However, the value decreased to be 5.86% in size scenario of 100 000 m^3, which is due to the lower hazard probability in size scenario 100 000 m^3. The same tendency also exists for the populations inside buildings. About 30 per cent population will be exposed to landslide in the 50 years return period.

Accordingly, eight vulnerability maps for buildings and eight vulnerability maps for populations inside buildings are created for the four return periods and two size scenarios. For example, Fig. 12 and Fig. 13 show the four resulting vulnerability maps for buildings and population inside the buildings under four return periods and the case of landslide volume equal to or greater than 50 000 m^3. The majority of exposed buildings are located on the slopes with high or very high hazard level, such as Caolinwan, Dafangping, Sanfangping villages. The buildings and population inside the buildings in these community centres are not exposed to slope hazard, thanks to the very low class (0-0.1) of landslide probability hazard.

As discussed in Table IV of Section 3.3, we assigned the vulnerability value to be 1.0 for buildings located on slopes. This causes the buildings outside the flat areas in the community show very high vulnerability value in Fig. 12. The vulnerability map shown in Fig. 12 was classified into five categories ranging from very low to very high. In the case of 50 years return period and 50 000 m^3 size scenario, there are 18% building areas with very high-class vulnerability. Vulnerability value of populations was then assigned according to Equation 4 in section 3.3 based on the building vulnerability result. The very-high class population vulnerability shown in Fig. 13 was over than 0.5, the area of which is about ten percent of the exposed people and mainly concentrates in the influence area of slopes in Dafangping, Caolinwan, Sanfangping or on the slopes which have the very-high class hazard probability assessed in Fig. 11.

https://doi.org/10.5194/nhess-2019-259
Preprint. Discussion started: 23 August 2019
© Author(s) 2019. CC BY 4.0 License.

Natural Hazards and Earth System Sciences
Discussions

Table VI. Exposure and risk of buildings and population for landslide under four return periods (5,10,20,50 years) and two size scenarios (landslide volume equal to or greater than 50 000 m³ or 100 000 m³) by using the methodology in Section 3.2 and 3.3. (Number in brackets are in percentage)

Size scenario		Volume >=50 000 m³				Volume >=100 000 m³			
Return Period(years)		5	10	20	50	5	10	20	50
Exposure	Population	0	0	4073(8.87%)	14257(31.05%)	0	0	2724(5.93%)	13746(29.94%)
	Building area(×10 000m²)	0	0	16.3(8.76%)	57(30.64%)	0	0	10.9(5.86%)	55(29.57%)
Risk	Casualties (person)	0	0	771(1.68%)	1485(3.23%)	0	0	584(1.27%)	1235(2.69%)
	Economic losses (×10 000 RMB)	0	0	6039(3.69%)	11629(7.10%)	0	0	4615(2.82%)	9352(5.71%)
Annual Risk	Casualties (person)	59(0.13%)				47(0.10%)			
	Economic losses (×10 000 RMB)	463(0.3%)				359(0.23%)			

https://doi.org/10.5194/nhess-2019-259
Preprint. Discussion started: 23 August 2019
© Author(s) 2019. CC BY 4.0 License.

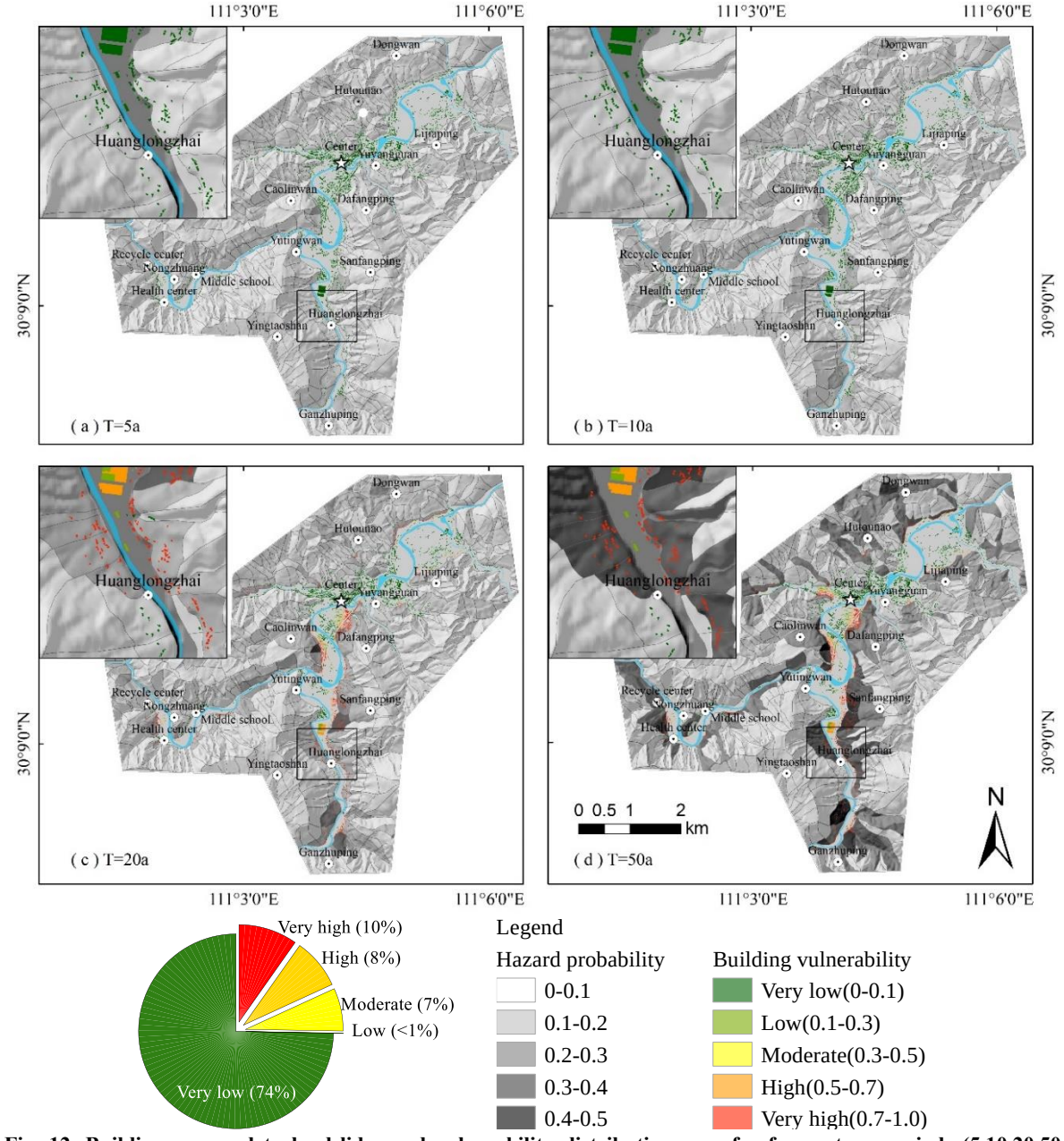

Fig. 12. Buildings exposed to landslides and vulnerability distribution map for four return periods (5,10,20,50 years) and size scenario of landslide volume equal to or greater than 50 000 m³.

https://doi.org/10.5194/nhess-2019-259
Preprint. Discussion started: 23 August 2019
© Author(s) 2019. CC BY 4.0 License.

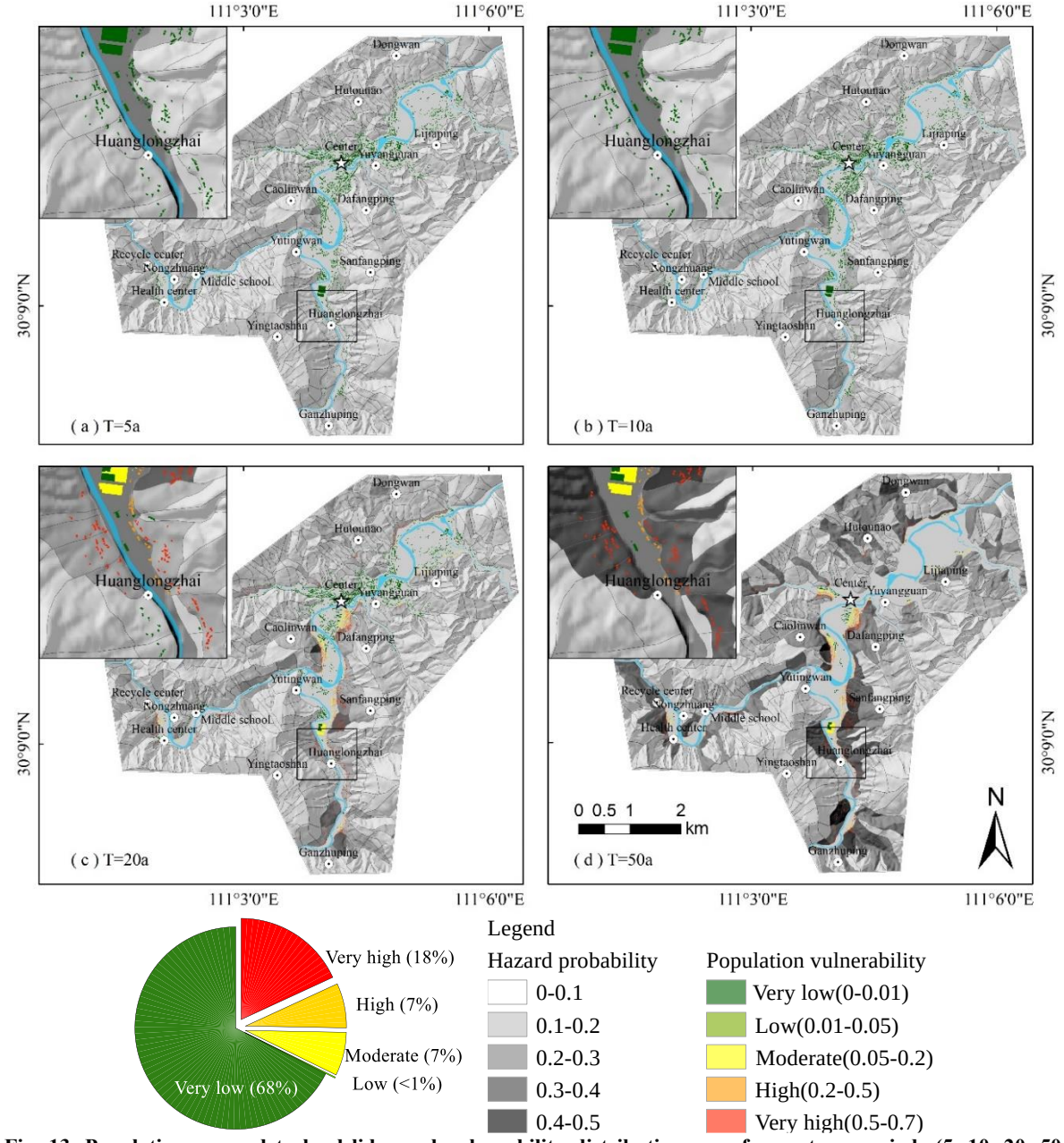

Fig. 13. Population exposed to landslides and vulnerability distribution map four return periods (5, 10, 20, 50 years) and size scenario of landslide volume equal to or greater than 50 000 m³.

https://doi.org/10.5194/nhess-2019-259
Preprint. Discussion started: 23 August 2019
© Author(s) 2019. CC BY 4.0 License.

Natural Hazards and Earth System Sciences Discussions

4.4 Risk assessment

Landslide risk maps were generated from the eight hazard maps, eight vulnerability maps and the value or amount of elements-at-risk by equation 5. An example of a risk map for the loss of population is shown in Fig. 14. The map created for 50 years return period for example (see Fig. 14d) shows that potential loss was concentrated in the urban and densely-populated areas along the Yuyangguan River, especially at the toe of the slope of Caolinwan, Dafangping, Sanfangping villages.

Table VI presents the final population and buildings risks for four return periods and two size scenarios. Accordingly, there are no potential losses in five and ten return years. The result of no risk in 5 year return period can be proved by the fact that no casualties or economic losses are reported in Yuyangguan community since 2014. For the case of volume equal to or greater than 50 000 m^3, however, the potential casualties are 771 persons, 1.68% of the total populations in the community. The economic losses are calculated as about 60 million RMB in 20 years return period, about 3.7% of buildings economic values. As shown in Table VI, the risk is expected to be double in the next 50 years return period. In the case of volume equal to or greater than 100 000 m^3, the potential loss will be lower. For example, there is 1.27% of the populations exposed to landslides, 0.41% lower than that in size scenario of 50 000 m^3.

https://doi.org/10.5194/nhess-2019-259
Preprint. Discussion started: 23 August 2019
© Author(s) 2019. CC BY 4.0 License.

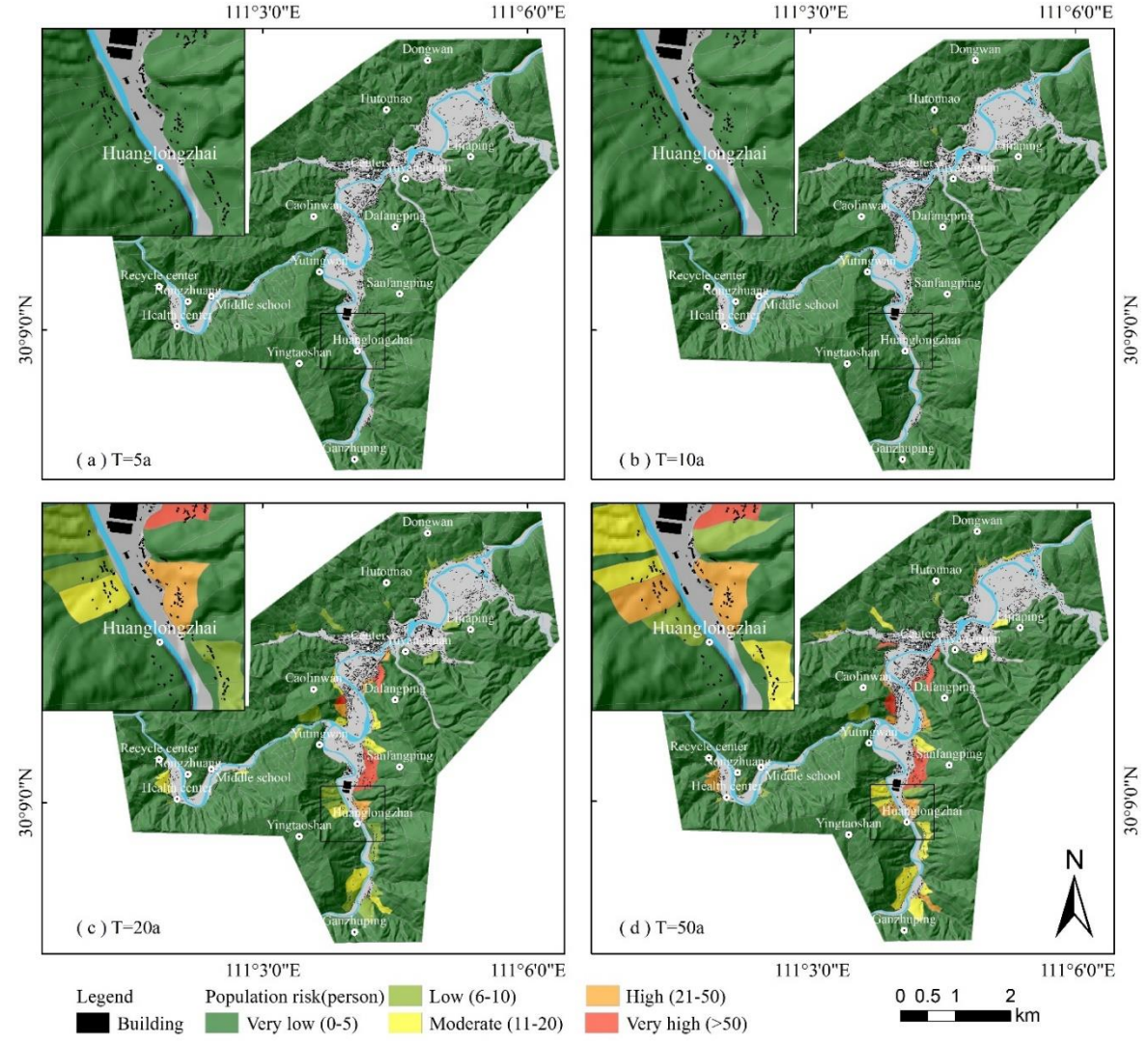

Fig. 14. Example of a risk map for the loss of population for four return periods (5, 10, 20, 50 years) and the landslide size scenario equal to or greater than 50 000 m³.

295

https://doi.org/10.5194/nhess-2019-259
Preprint. Discussion started: 23 August 2019
© Author(s) 2019. CC BY 4.0 License.

Natural Hazards and Earth System Sciences Discussions

5. DISCUSSION

5.1. Discussion on landslide susceptibility map

Landslide susceptibility result shows that lithology is the most important controlling factor. Quaternary eluvium (Q_4^{dl+el}) and Guniutan limestone from Ordovician (O_2g) has the top two weight values in the susceptibility map. It is consistent with the findings in fieldwork by the authors. Residual deposit and eluvium is the composition of clay and gravels, which is with low strength and is the main areas with intensive human activities in Yuyangguan community. As to the bedrock O_2g, it is with high strength and not vulnerable to have a landslide. But in the field, we found two groups of joint surface in O_2g, which are the vital in understanding why the YYG07 landslide occurred (see Table II). We can also find in the field that the majority of landslides occurred in Silurian sandstone and shale. However, the weight value (0.3) of *S* is lower than the value of Q_4^{dl+el} and O_2g. This is because that although more landslides occurred in Silurian sandstone and shale, but the area of Silurian formation is much larger in Yuyangguan community (see Fig. 1). Therefore, we should take the things in mind that slopes in Ordovician limestone can have a much high landslide probability and we should pay attention to the slopes although historical landslides are not too much now.

5.2. Discussion on landslide hazard assessment

Landslide hazard maps are generated for four assumed return periods (5, 10, 20, and 50 years) and two size scenarios. Theoretically, the definition of hazard scenarios as described by Chen et al. (2016b).should be based on the analysis of landslide occurrences and triggering events. due to the incomplete information on landslide date in the community, it is challenging to build the relationship between landslide return period and triggering factor (rainfall in this case study). However, we find that since 2014 no landslide occurred in Yuyangguan community, which is consistent with the hazard result in 5-year return period (see Fig. 11a). It means that the way of temporal probability using the Poisson model is feasible for landslide hazard assessment when a landslide database incomplete with detail occurrence date and triggering event data(such as rainfall).

In size probability analysis, the landslide probability distribution is key for quantifications. We found that the classical distribution model (Malamud et al., 2004;Stark and Hovius, 2001) did not show an excellent fitting performance in this study. The difference in landslide size between Malamud's and our landslide database is the main reason. No small landslides (< 1000 m^2 in Malamud's research) are presented or recorded in Yuyangguan community. The simulated equation (in Fig. 9) is suitable for landslide risk assessment in this research. In future, however, comparison with the classical models should still be taken with a more complete database or more landslide events.

5.3. Other limitations in risk results

Uncertainties do exist in the final risk maps due to some other items, such as element at risk data and its vulnerability or resilience. In this study, we get the data of buildings and population inside the buildings at risk by empirical calculation for

https://doi.org/10.5194/nhess-2019-259
Preprint. Discussion started: 23 August 2019
© Author(s) 2019. CC BY 4.0 License.

Natural Hazards and Earth System Sciences Discussions

landslide influence area. Further study will be taken by numerical modelling considering landslide material, pore water pressure and ground surface characteristic besides slope height and volume used in this paper.

Meanwhile, the risk results cannot be tested because of the lack of historical damage data in the area, which is a common difficulty in China and other researcher's areas(Ghosh et al., 2011;Chen et al., 2016b). Damage data is also crucial for vulnerability analysis. We considered building typology and location to landslide to assess the physical vulnerability based on local experts' opinion. However, the resilience of element-at-risk can contribute to a reasonable decrease in vulnerability. The mobility of persons and their characteristics (such as age, education, physical disability) and disaster prevention capability of the government were not taken into consideration in the community. In future, physical vulnerability curves for buildings and population are urgent to be constructed in the area.

From susceptibility to risk assessment, we hold the assumption that landslide will occur under the same condition which caused historical landslides. However, morphometric, geo-environmental conditions and assets will change in practice. Despite this, the resulting maps can be referred for landslide risk controlling strategy making and land use planning in Yuyangguan community. Risk controlling measurements can be planned on each slope unit using a matrix from the combination of landslide hazard probability and risk maps. For example, risk management on slope units with very high-class hazard probability and very high-risk can be suggested as relocation or engineering works, while the slopes with high-class hazard probability and mid-class risk suggested being monitored by GPS or borehole inclinometer. Also, the four return periods and two size scenarios can be used for multi-temporal land use planning, such as short term (in 5 years), mid-term (10-20years) and long-term(50 years). The annual risk value on each slope can be used for cost-benefit analysis in risk decision. To some extent, it answers the question raised by Guzzetti et al. (2005) that how to combine a large number of hazard maps efficiently for different users.

6. CONCLUSIONS

We conducted a semiquantitative risk assessment for landslides at a community scale based on the definition of landslide risk given by Varnes and the IAEG (1984). In our case study, we focused on the potential loss of building and populations inside buildings. We generated one susceptibility map, eight hazard maps, eight vulnerability maps and eight risk maps for four return periods(5,10,20,50 years) and two size scenarios(equal to or greater than 50 000 m^3 and equal to or greater than 100 000 m^3). The landslide susceptibility result was tested to have a success rate of 0.84 and indicates the important contribution of Quaternary eluvium, Guniutan limestone from Ordovician. The way of generating hazard maps by integrating three probabilities (spatial, temporal and size probability) proved applicable in this case study area. While in size probability calculation, a normal distribution function of landslide should be used carefully and better fitting function is suggested to be found if small landslide data are scarce in the area. Also, landslide influence area can be empirically determined at a community scale by using simple data (slope height an volume) if geotechnical parameters not available. However, for more accurate vulnerability assessment, numerical modelling on landslide travel distance is suggested because the resulting intensity parameters, such as velocity, depth are essential input data for vulnerability quantification. Besides the

https://doi.org/10.5194/nhess-2019-259
Preprint. Discussion started: 23 August 2019
© Author(s) 2019. CC BY 4.0 License.


presented limitations, we believe that the proposed risk maps can tell the local stakeholders how to make different period of risk planning for the total community, such as short term (in 5 years), mid-term (10-20years) and long-term (50 years) strategy, or provide the reference to do cost-benefit analysis for each slope unit from the result of quantified annual risk value.

Data availability.

We thank China Geological Survey for the data for this work. Unluckily, the data is not available unless get the permission from China Geological Survey.

Author contribution.

Yin, Chen, Xu, Lian and Li supervised the field work and collected the complicated data. Chen and Fu discussed the whole plan of this article, designed and implemented all the experiments. Fu prepared all the data and finish the draft, including all figures in the article. Chen and Woldai revised the article. Du and Zhou supported the methods and techniques.

Competing interests.

The authors declare that they have no conflict of interest.

Special issue statement.

This research article is part of the special issue “Advances in extreme value analysis and application to natural hazards”. The article is not associated with a conference.

Acknowledgment

The research was supported by the National Natural Science Foundation of China (No. 41877525; No. 41641012), and the Research Foundation of Guideline for Geological Hazards in Mountainous Towns in Wuling Area, D5.7.3, China Geological Survey. The authors appreciate the support.

References

Abdulwahid, W. M., and Pradhan, B.: Landslide vulnerability and risk assessment for multi-hazard scenarios using airborne laser scanning data (LiDAR), Landslides, 14, 1057-1076, 10.1007/s10346-016-0744-0, 2016.

Ayalew, L., Yamagishi, H., and Ugawa, N.: Landslide susceptibility mapping using GIS-based weighted linear combination, the case in Tsugawa area of Agano River, Niigata Prefecture, Japan, Landslides, 1, 73-81, 10.1007/s10346-003-0006-9, 2004.

Chen, H. X., Zhang, S., Peng, M., and Zhang, L. M.: A physically-based multi-hazard risk assessment platform for regional rainfall-

© Author(s) 2019. CC BY 4.0 License.

induced slope failures and debris flows, Engineering Geology, 203, 15-29, 10.1016/j.enggeo.2015.12.009, 2016a.

Chen, L., Yin, K. L., and Dai, Y. X.: Building vulnerability evaluation in landslide deformation phase, Journal of Mountain Science, 8, 286-295, 10.1007/s11629-011-2101-z, 2011.

Chen, L., van Westen, C. J., Hussin, H., Ciurean, R. L., Turkington, T., Chavarro-Rincon, D., and Shrestha, D. P.: Integrating expert opinion with modelling for quantitative multi-hazard risk assessment in the Eastern Italian Alps, Geomorphology, 273, 150-167, 10.1016/j.geomorph.2016.07.041, 2016b.

Corominas, J.: The angle of reach as a mobility index for small and large landslides, Canadian Geotechnical Journal, 33, 260-271, 1996.

Crovelli, R. A.: Probability models for estimation of number and costs of landslides, U.S. Geological Survey, 2000.

Cruden, D. M.: A simple definition of a landslide, Bulletin of the International Association of Engineering Geology, 43, 27-29, 10.1007/bf02590167, 1991.

Erener, A., and Düzgün, H. B. S.: A regional scale quantitative risk assessment for landslides: case of Kumluca watershed in Bartin, Turkey, Landslides, 10, 55-73, 10.1007/s10346-012-0317-9, 2012.

Erener, A., Mutlu, A., and Sebnem Düzgün, H.: A comparative study for landslide susceptibility mapping using GIS-based multi-criteria decision analysis (MCDA), logistic regression (LR) and association rule mining (ARM), Engineering Geology, 203, 45-55, 10.1016/j.enggeo.2015.09.007, 2016.

Fell, R., Corominas, J., Bonnard, C., Cascini, L., Leroi, E., and Savage, W. Z.: Guidelines for landslide susceptibility, hazard and risk zoning for land-use planning, Engineering Geology, 102, 99-111, 10.1016/j.enggeo.2008.03.014, 2008a.

Fell, R., Corominas, J., Bonnard, C., Cascini, L., Leroi, E., and Savage, W. Z.: Guidelines for landslide susceptibility, hazard and risk zoning for land use planning, Engineering Geology, 102, 85-98, 10.1016/j.enggeo.2008.03.022, 2008b.

Ghosh, S., van Westen, C. J., Carranza, E. J. M., and Jetten, V. G.: Integrating spatial, temporal, and magnitude probabilities for medium-scale landslide risk analysis in Darjeeling Himalayas, India, Landslides, 9, 371-384, 10.1007/s10346-011-0304-6, 2011.

Gokceoglu, C., and Aksoy, H.: Landslide susceptibility mapping of the slopes in the residual soils of the Mengen region (Turkey) by deterministic stability analyses and image processing techniques, Engineering Geology, 44, 147-161, 1996.

Guzzetti, F., Reichenbach, P., Cardinali, M., Galli, M., and Ardizzone, F.: Probabilistic landslide hazard assessment at the basin scale, Geomorphology, 72, 272-299, 10.1016/j.geomorph.2005.06.002, 2005.

Guzzetti, F., Galli, M., Reichenbach, P., Ardizzone, F., and Cardinali, M.: Landslide hazard assessment in the Collazzone area, Umbria, Central Italy, Natural Hazards and Earth System Sciences, 6, 115-131, https://doi.org/10.5194/nhess-6-115-2006, 2006.

Guzzetti, F., Mondini, A. C., Cardinali, M., Fiorucci, F., Santangelo, M., and Chang, K.-T.: Landslide inventory maps: New tools for an old problem, Earth-Science Reviews, 112, 42-66, 10.1016/j.earscirev.2012.02.001, 2012.

Hong, H., Ilia, I., Tsangaratos, P., Chen, W., and Xu, C.: A hybrid fuzzy weight of evidence method in landslide susceptibility analysis on the Wuyuan area, China, Geomorphology, 290, 1-16, 10.1016/j.geomorph.2017.04.002, 2017.

Huang, F., Yin, K., Huang, J., Gui, L., and Wang, P.: Landslide susceptibility mapping based on self-organizing-map network and extreme learning machine, Engineering Geology, 223, 11-22, 10.1016/j.enggeo.2017.04.013, 2017.

Hungr, O., Fell, R., Couture, R., and Eberhardt, E.: Landslide risk management, Taylor and Francis, London, 2005.

Jiménez-Perálvarez, J. D., El Hamdouni, R., Palenzuela, J. A., Irigaray, C., and Chacón, J.: Landslide-hazard mapping through multi-technique activity assessment: an example from the Betic Cordillera (southern Spain), Landslides, 14, 1975-1991, 10.1007/s10346-017-0851-6, 2017.

Lee, S., Ryu, J.-H., and Kim, I.-S.: Landslide susceptibility analysis and its verification using likelihood ratio, logistic regression, and artificial neural network models: case study of Youngin, Korea, Landslides, 4, 327-338, 10.1007/s10346-007-0088-x, 2007.

Li, Z., Nadim, F., Huang, H., Uzielli, M., and Lacasse, S.: Quantitative vulnerability estimation for scenario-based landslide hazards, Landslides, 7, 125-134, 10.1007/s10346-009-0190-3, 2010.

Liu, Y., Yin, K., Chen, L., Wang, W., and Liu, Y.: A community-based disaster risk reduction system in Wanzhou, China, International Journal of Disaster Risk Reduction, 19, 379-389, 10.1016/j.ijdrr.2016.09.009, 2016.

Malamud, B. D., Turcotte, D. L., Guzzetti, F., and Reichenbach, P.: Landslide inventories and their statistical properties, Earth Surface Processes and Landforms, 29, 687-711, 10.1002/esp.1064, 2004.

Mavrouli, O., Corominas, J., Ibarbia, I., Alonso, N., Jugo, I., Ruiz, J., Luzuriaga, S., and Navarro, J. A.: Integrated risk assessment due to slope instabilities in the roadway network of Gipuzkoa, Basque Country, Natural Hazards and Earth System Sciences, 19, 399-419, 10.5194/nhess-19-399-2019, 2019.

McAdoo, B. G., Quak, M., Gnyawali, K. R., Adhikari, B. R., Devkota, S., Rajbhandari, P. L., and Sudmeier-Rieux, K.: Roads and landslides in Nepal: how development affects environmental risk, Natural Hazards and Earth System Sciences, 18, 3203-3210, 10.5194/nhess-18-3203-2018, 2018.

Mennis, J.: Generating Surface Models of Population Using Dasymetric Mapping, PROFESSIONAL GEOGRAPHER, 55, 31-42, 2003.

Metz, C. E.: Basic principles of ROC analysis, Seminars in Nuclear Medicine, 8, 283-298, 1978.

Neuhäuser, B., and Terhorst, B.: Landslide susceptibility assessment using “weights-of-evidence” applied to a study area at the

https://doi.org/10.5194/nhess-2019-259
Preprint. Discussion started: 23 August 2019
© Author(s) 2019. CC BY 4.0 License.

Jurassic escarpment (SW-Germany), Geomorphology, 86, 12-24, 10.1016/j.geomorph.2006.08.002, 2007.

Paliaga, G., Faccini, F., Luino, F., and Turconi, L.: A spatial multicriteria prioritizing approach for geo-hydrological risk mitigation planning in small and densely urbanized Mediterranean basins, Natural Hazards and Earth System Sciences, 19, 53-69, 10.5194/nhess-19-53-2019, 2019.

Peduto, D., Ferlisi, S., Nicodemo, G., Reale, D., Pisciotta, G., and Gullà, G.: Empirical fragility and vulnerability curves for buildings exposed to slow-moving landslides at medium and large scales, Landslides, 14, 1993-2007, 10.1007/s10346-017-0826-7, 2017.

Qiao, S., Qin, S., Chen, J., Hu, X., and Ma, Z.: The Application of a Three-Dimensional Deterministic Model in the Study of Debris Flow Prediction Based on the Rainfall-Unstable Soil Coupling Mechanism, Processes, 7, 99, 10.3390/pr7020099, 2019.

Quan Luna, B., Blahut, J., Van Westen, C. J., Sterlacchini, S., Van Asch, T. W. J., and Akbas, S. O.: The application of numerical debris flow modelling for the generation of physical vulnerability curves, Natural Hazards and Earth System Science, 11, 1-14, 10.5194/nhess-11-1-2011, 2011.

Stark, C. P., and Hovius, N.: The characterization of landslide size distributions, Geophysical Research Letters, 28, 1091-1094, 10.1029/2000gl008527, 2001.

Van Westen, C. J., Van Asch, T. W. J., and Soeters, R.: Landslide hazard and risk zonation—why is it still so difficult?, Bulletin of Engineering Geology and the Environment, 65, 167-184, 10.1007/s10064-005-0023-0, 2005.

Van Westen, C. J., Castellanos, E., and Kuriakose, S. L.: Spatial data for landslide susceptibility, hazard, and vulnerability assessment: An overview, Engineering Geology, 102, 112-131, 10.1016/j.enggeo.2008.03.010, 2008.

Van Westen, C. J., and Greiving., S.: Environmental Hazards Methodologies for Risk Assessment and Management, International Water Association Publishing, London, 2017.

Varnes: Landslide hazard zonation: a review of the principles and practice, Scientific and Cultural Organization, Paris, 1984.

Zezere, J. L., Pereira, S., Melo, R., Oliveira, S. C., and Garcia, R. A. C.: Mapping landslide susceptibility using data-driven methods, Sci Total Environ, 589, 250-267, 10.1016/j.scitotenv.2017.02.188, 2017.